LAWRENCE
LIVERMORE
NATIONAL
LABORATORY

UCRL-TR-214827

Modeling the Effects of (lambda)-gun on SSPX Operation: Mode Spectra, Internal Magnetic Field Structure, and Energy Confinement

E.B. Hooper

August 25, 2005

This work was performed under the auspices of the U.S. Department of Energy by University of California, Lawrence Livermore National Laboratory under Contract W-7405-Eng-48.

Modeling the effects of λ_{gun} on SSPX operation: Mode spectra, internal magnetic field structure, and energy confinement

E. B. Hooper

Fusion Energy Program, Physics and Advanced Technologies Directorate
Lawrence Livermore National Laboratory
Livermore, CA 94550

August 23, 2005

Abstract

The Sustained Spheromak Physics Experiment (SSPX) shows considerable sensitivity to the value of the injected ("gun") current, I_{gun}, parameterized by the relative values of $\lambda_{gun} = \mu_0 I_{gun} / \Psi_{gun}$ (with Ψ_{gun} the bias poloidal magnetic flux) to the lowest eigenvalue of $\nabla \times \mathbf{B} = \lambda_{FC}\mathbf{B}$ in the flux conserver geometry. This report discusses modeling calculations using the NIMROD resistive-MHD code in the SSPX geometry. The behavior is found to be very sensitive to the profile of the safety factor, *q*, with the excitation of interior MHD modes at low-order resonant surfaces significantly affecting the evolution. Their evolution affects the fieldline topology (closed flux, islands, stochastic fieldlines confined by KAM surfaces, and open fieldlines), and thus electron temperature and other parameters. Because of this sensitivity, a major effect is the modification of the *q*-profile by the current on the open fieldlines in the flux core along the geometric axis. The time-history of a discharge can thus vary considerably for relatively small changes in I_{gun}. The possibility of using this sensitivity for feedback control of the discharge evolution is discussed, but modeling of the process is left for future work.

I. Introduction

The plasma quality in SSPX shows a clear sensitivity on the ratio of current to bias poloidal flux of the helicity injector ("gun"),[1] as measured, e.g., by the peak electron temperature or the magnetic fluctuation amplitude and mode number. This ratio is expressed as

$$\lambda_{gun} = \mu_0 I_{gun} / \Psi_{gun} \tag{1}$$

The natural measure of this quantity is the lowest eigenvalue of $\nabla \times \mathbf{B} = \lambda_{FC}\mathbf{B}$ in the flux conserver geometry. In SSPX λ_{FC}=9.6 m^{-1}.

The purpose of the present note is to explore this sensitivity and related effects using the NIMROD code and to provide comparisons between modeling results and the experiment. It builds on and documents in detail results also seen in Refs. [2,3,4] (These papers, and references therein, describe the code, boundary conditions, etc.) The sensitivity is also documented in viewgraphs presented at a NIMROD workshop,[5] including using different gun currents and toroidal flux

and appears to be quite general. We will see that the code results are as sensitive as the experiment to small variations in the ratio of the gun-lambda to the flux conserver eigenvalue. It appears that a major contribution to the sensitivity arises from evolutionary variations in the q-profile and the resultant fluctuation spectrum and plasma structure. As an extreme example are results with λ_{gun} = 8.1 m^{-1}, held constant in time after an initial formation. Late in time there is only one mode of significant amplitude, n=4 (with m=2). Its amplitude is small, $\delta B/B \approx 0.1\%$ at the midplane magnetic probe position, but the magnetic structure inside the separatrix has significant islands which must be playing a large role in confinement. (Fieldlines are confined and apparently not chaotic for this example.) The temperature profile in a poloidal plane has a noticeable quadrupole structure but no islands. In other cases, e.g. at higher λ_{gun}, the temperature profile is less symmetric and may have islands or large regions of nearly constant temperature in regions of chaotic fieldlines, and probably corresponds to some of the flat-topped and other spatial variations seen in the Thomson scattering results.

This note starts with a brief discussion of some pertinent experimental results. Following this is a comparison of two computational results which used the time history of the current used in the experiment. These modeling results reproduce many of the experimental observations, as discussed in two recent publications.[2, 3] There are also differences between the two simulations and with experiment, including the profile of $\lambda = \mu_0 \mathbf{j}\cdot\mathbf{B}/B^2$ on the open fieldlines in the flux core around the geometric axis. The differences are reflected in the profile of the safety factor, q, inside the separatrix and thus in the amplitudes of magnetic modes in the spheromak.

To further explore this observation, a series of simulations was undertaken varying the value of λ_{gun}. These are presented in the fourth section and reveal significant variation in the field structure in the spheromak as a function of λ_{gun} and as a function of time at constant λ_{gun}. The structures under various conditions may include good, closed flux surfaces; magnetic islands; confined chaotic fieldlines; and/or open lines which reach the electrodes. These structures correlate with the magnetic fluctuation modes and have strong effects on the electron temperature magnitude and profile.

We conclude the note with a summary of results and the lessons which these have for experiments in SSPX. The possibility of using the gun current to optimize the q-profile is briefly explored.

II. Some results from SSPX

The sensitivity of the plasma to λ_{gun} is apparent from the peak electron temperature achieved in a series of discharges at fixed gun current but varying bias flux, as shown in Fig. 1. Note that the peak temperature is for $\lambda_{gun} < \lambda_{FC}$.

The highest temperatures in the experiment correspond to temperature profiles that are peaked and have widths comparable to the width of the spheromak separatrix as determined by fitting magnetic probe data to the Grad-Shafranov equation using the Corsica code. An example is shown in Fig. 2 together with the safety-factor (q) profile from the fit. The fits for discharges with high T_e find flat λ on the open fieldlines in the flux core. Experimental magnetic

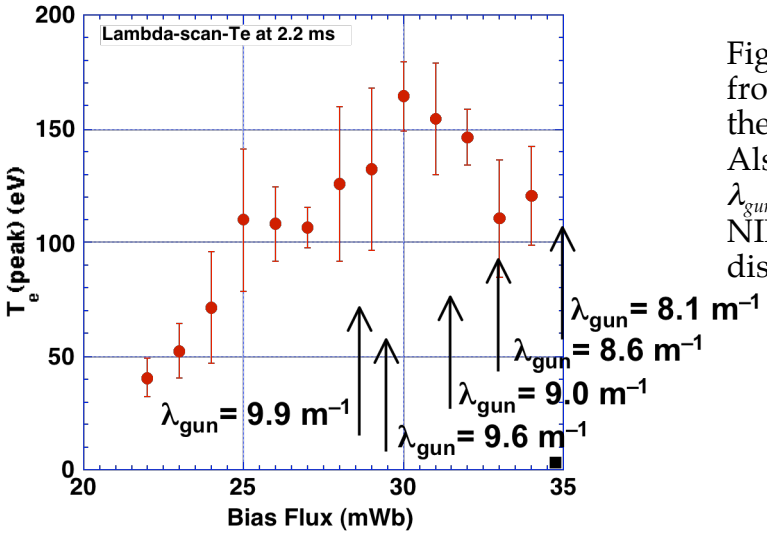

Fig. 1. Peak temperatures from an experimental scan of the gun flux (and thus λ_{gun}). Also shown are the values of λ_{gun} used in a series of NIMROD simulations discussed later in this note.

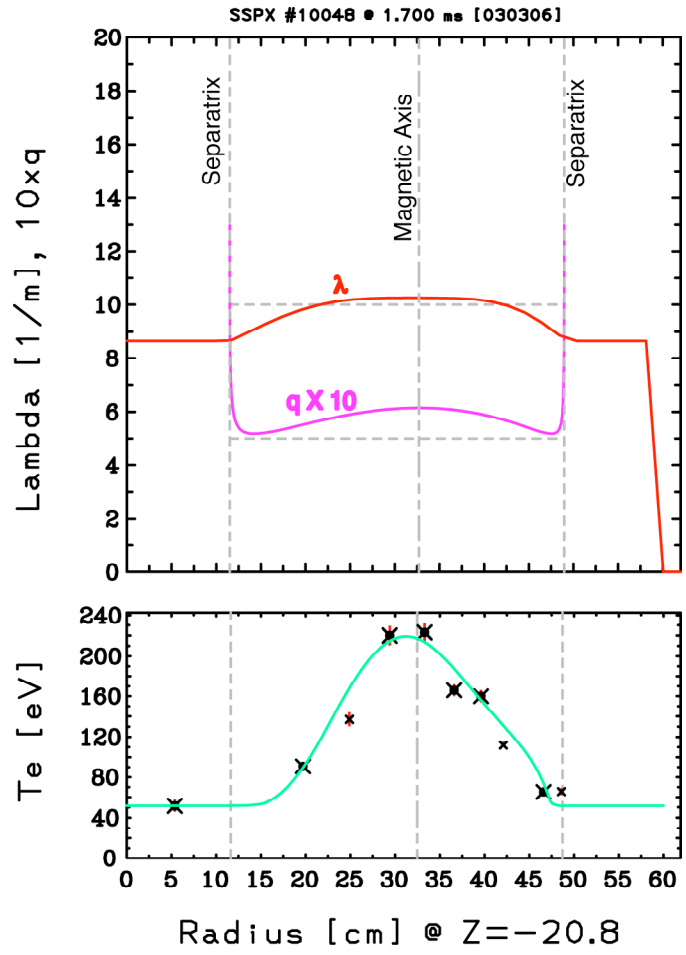

Fig. 2. Example of a peaked, experimental temperature profile and corresponding q profile from SSPX.[6]

fluctuation levels are low and mode numbers are consistent with low rational values of the q-profile.[6] At the ohmic power levels discussed in this report, electron temperatures greater than 200 eV have been obtained with rms fluctuation levels of ~ 1% at the flux conserver and the time at which the

Thomson scattering measurement is made. Ion temperatures are not known, but the electron-ion equilibration time at 150-200 eV and 7.5×10^{19} m^{-3} (typical of the experiment) is > 0.5 ms so the ions may be cooler than the electrons.

III. Simulations using the experimental time history of the gun current

Two simulations (*lam06* and *lam07*) have used the experimental time history for the current. The thermal conductivity used the parallel electron (temperature dependent) coefficient and the perpendicular thermal conductivity was set to 21 m^2/s in *lam06* and to ion-classical (temperature dependent) in *lam07*. The simulations differed in several ways, including the values of kinetic viscosity and the initial (t = 0) amplitudes of the toroidal Fourier modes. Also, in *lam06* the current late in the formation part of the current pulse began to increase due to a programming error. It was corrected from 498 kA to 280 kA at 0.327 ms. The immediate effect of this on the gun current profile is discussed below. Following this correction the gun current tracked the experiment accurately and the evolution of magnetic modes and flux and the electron temperature tracked the experiment quite well out to about 4 ms when the plasma collapsed in both simulation and experiment.[3] The *lam07* simulation had a similar time history but a higher magnetic field and fluctuation spectral histories which were somewhat different than *lam06*. It is instructive for our later discussion to compare (Fig. 3) the azimuthally averaged λ and q-profiles for the two simulations.

Two differences are immediately noticeable: (1) In *lam06*, λ has a small value (< 0.8 m^{-1}) on the geometric axis but in *lam07* it is large there (> 13 m^{-1}); and (2) The q-profile inside the separatrix ranges from 0.3 to 0.6 in *lam06* but 0.5 to 0.9 in *lam07*. The two results are related as the structure of the eigenmode in the flux-conserver geometry constrains the range of λ and the q-profile derives from λ.[7]

It is also interesting to compare the poloidal current and flux; cf. Fig. 4. The poloidal current response to the abrupt change of the gun current in *lam06* is shown in Fig. 5. Although there are some quantitative changes in the distribution of current on the cathode, it is not apparent how these would lead to the significant changes seen later in time, e.g. as in Fig. 4.

We conclude from these two simulations that the NIMROD results are in generally good agreement with the experiment, but that details matter when it comes to detailed, quantitative comparison. Both simulation and experiment are sensitive to the precise strength of the spheromak drive. In addition, the simulations yield peak electron temperatures that are about 60% of the experimental results, for reasons that are not presently clear.[3] We are consequently motivated to examine additional simulation results with the goal of better understanding the differences with experiment and their implications for the physics of the spheromak. In particular, we vary the value of λ_{gun} in the series of simulations discussed in the next section.

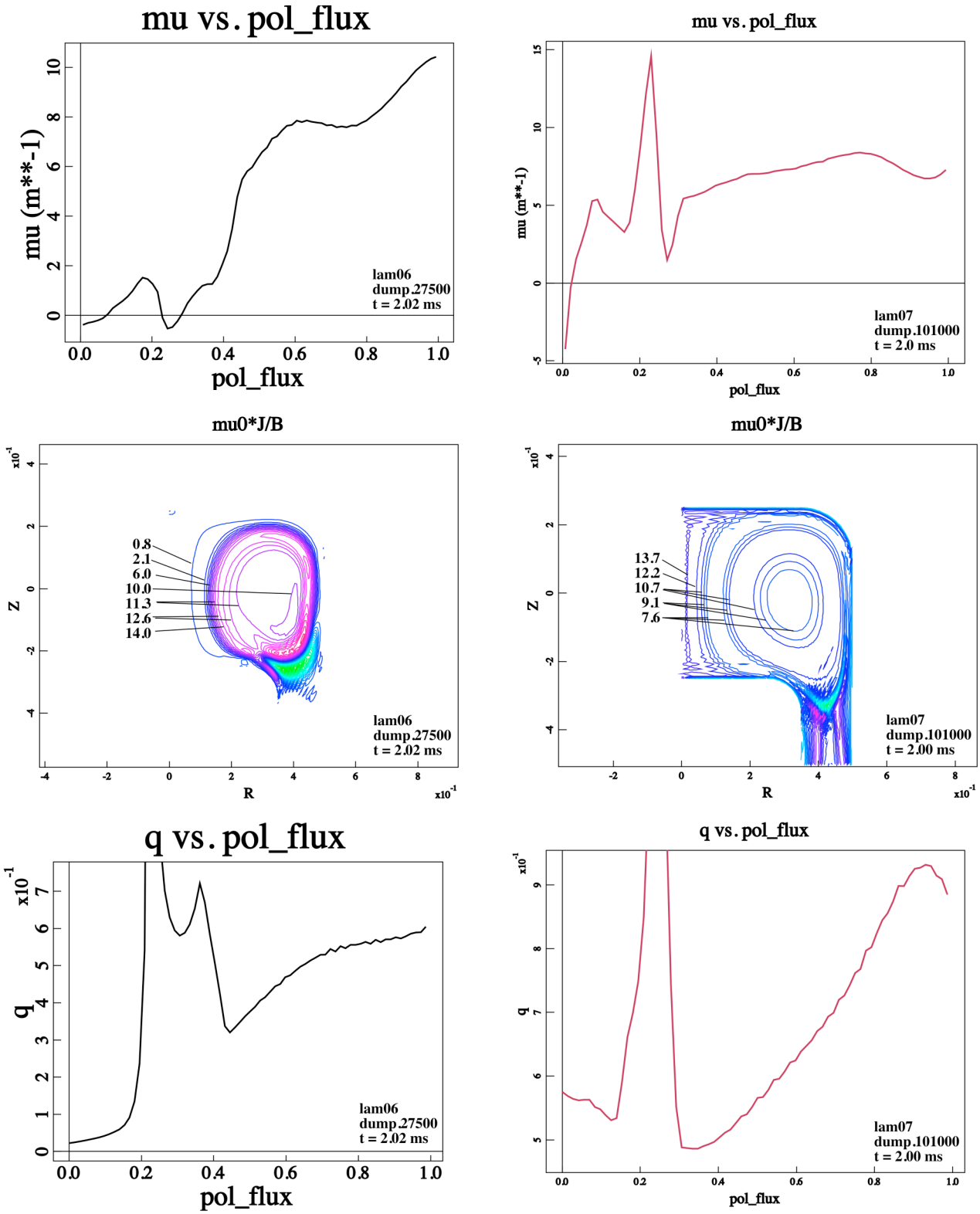

Fig. 3. Profiles of λ ("mu") and q. These are azimuthally averaged and the plots versus poloidal flux include points throughout the flux conserver and gun and thus differ from those found from a cut across the contours. Results from *lam06* are on the left and from *lam07* on the right. The poloidal flux is normalized to 1 at the magnetic axis.

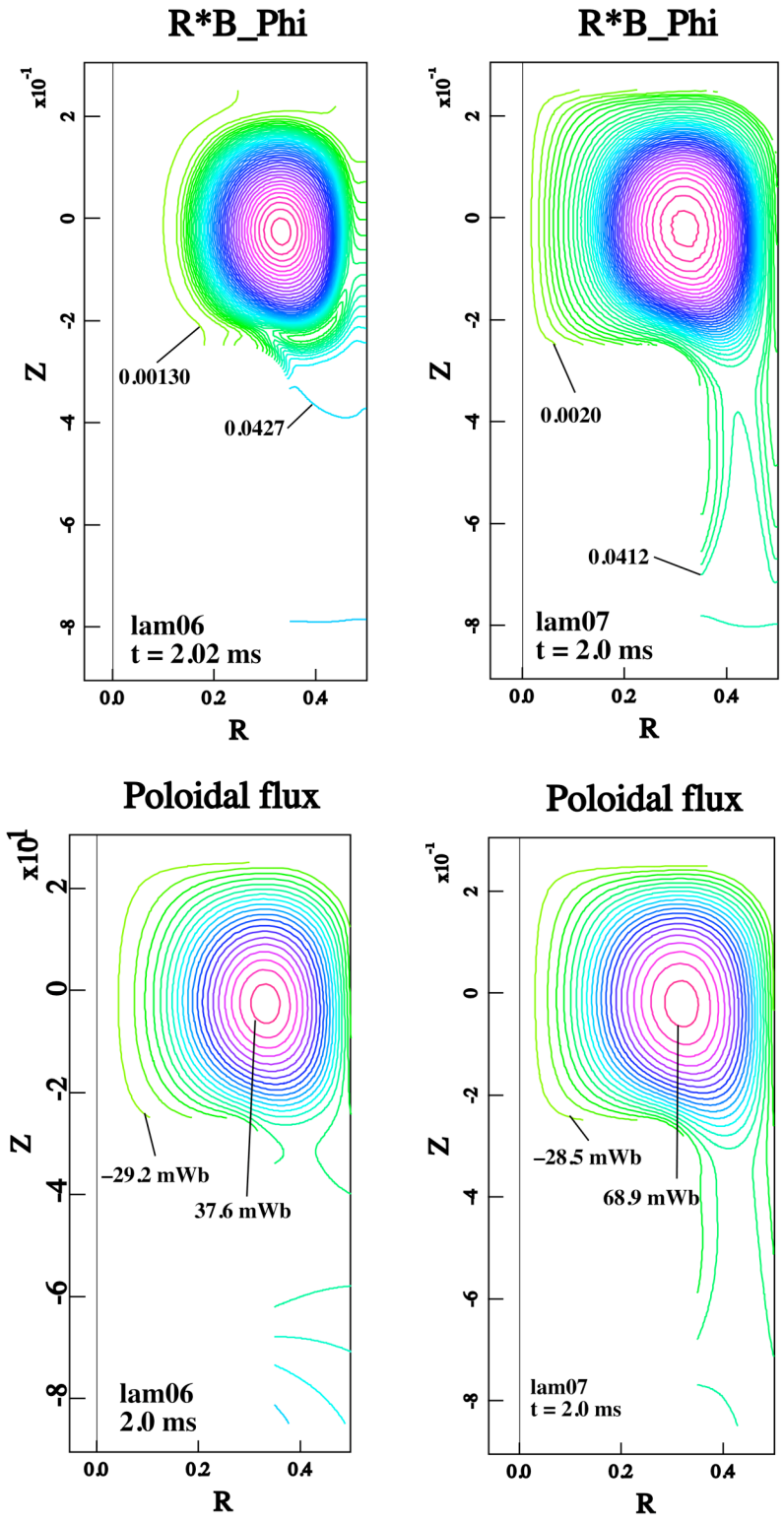

Fig. 4. Azimuthally-averaged poloidal current (I_{pol} =5R*B_phi in MA) and poloidal flux for *lam06* and *lam07*. Note the different current distributions along the surface of the gun even though the total gun currents are the same. The negative poloidal flux on the geometric axis corresponds to the applied bias flux. *lam07* has significantly greater flux amplification.

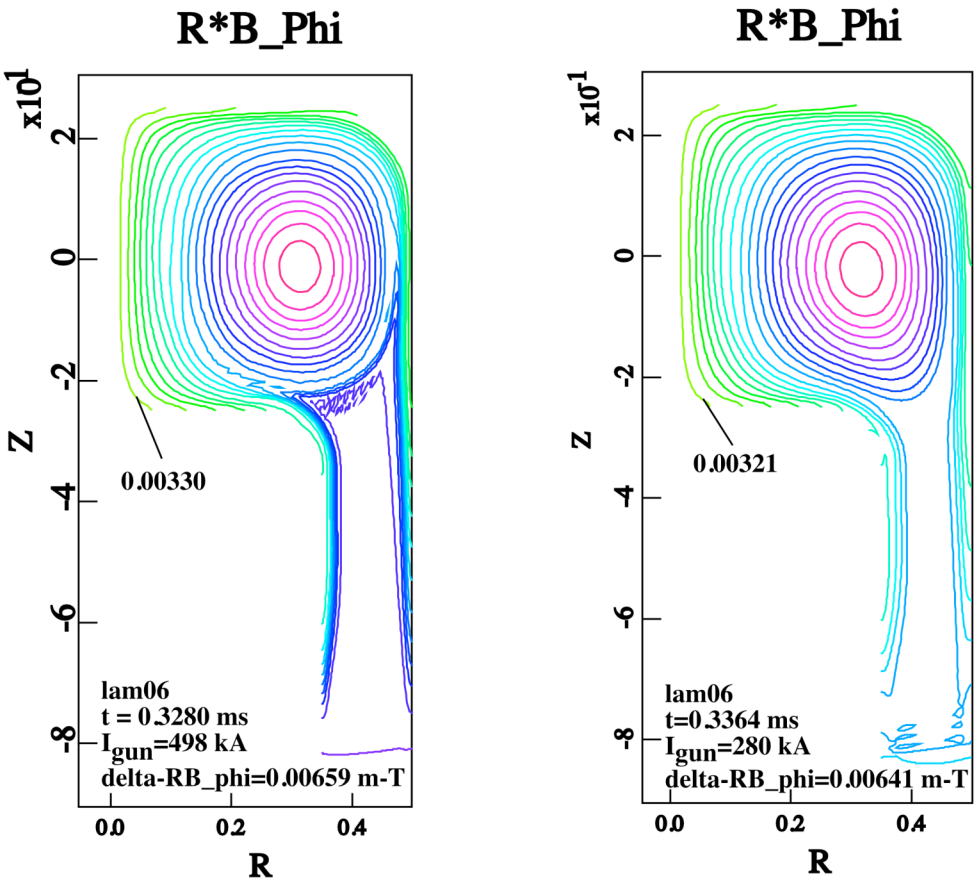

Fig. 5. Change in poloidal gun current distribution from the correction applied to *lam06* at 0.3289 ms.

IV. Exploring the sensitivity to λ_{gun}

We see that both experiment and simulations suggest that the detailed characteristics of the spheromak plasma are sensitive to the gun current and its spatial profile, even though the azimuthally-averaged flux geometry and time histories are surprisingly insensitive. To explore this, a series of simulations was run with the same initial plasma, generated by the formation pulse in the *lam07* simulation. For these simulations, the cross-field thermal conductivity was set to the ion-classical value. At five different times following the formation (0.37 ms < t < 0.48 ms) the gun current was fixed and held constant until the poloidal flux decayed to a level close to the bias value and the region of closed, azimuthally-averaged poloidal flux contours became small. An example is shown in Fig. 6 and the parameters are shown in Table 1.

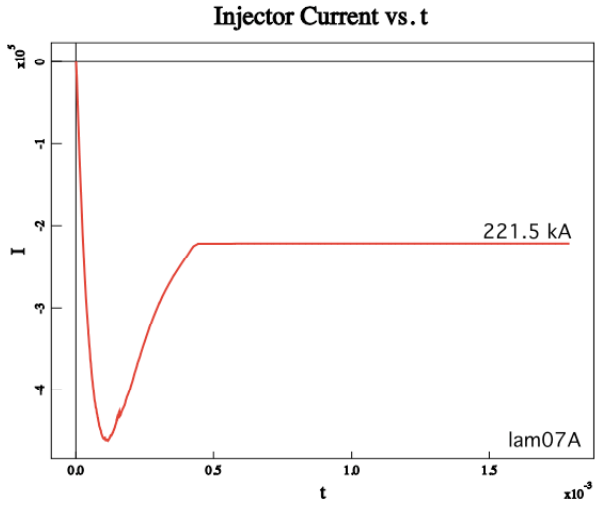

Fig. 6. An example of the gun-current time history for the sensitivity scan. Five simulations were conducted with 8.1 $m^{-1} \le \lambda_{gun} \le$ 9.9 m^{-1} during the constant-gun current phase as shown in Table 1 and in Fig. 1. The gun flux was constant at 31 mWb for all cases, and the formation currents were identical until held constant.

Simulation	**I_{gun} (kA)**	**λ_{gun} (m^{-1})**
Lam07B	200.0	8.1
Lam07E	212.0	8.6
Lam07A	221.5	9.0
Lam07D	237.0	9.6
Lam07C	243.8	9.9

Table 1. Simulations at constant gun current.

For each of these simulations there is a complex feedback between the plasma magnetic field, profiles of λ and q, MHD mode activity, and thermal losses that determines the detailed time evolution of the plasma. A chart describing some of these feedbacks is shown in Fig. 7, and helps guide understanding of the subsequent results.

Time history of λ_{gun} = 9.0. It is instructive first to examine one time history in detail as it illustrates the processes and results described in Fig. 7. The time evolution of *lam07A* is shown in Fig. 8.

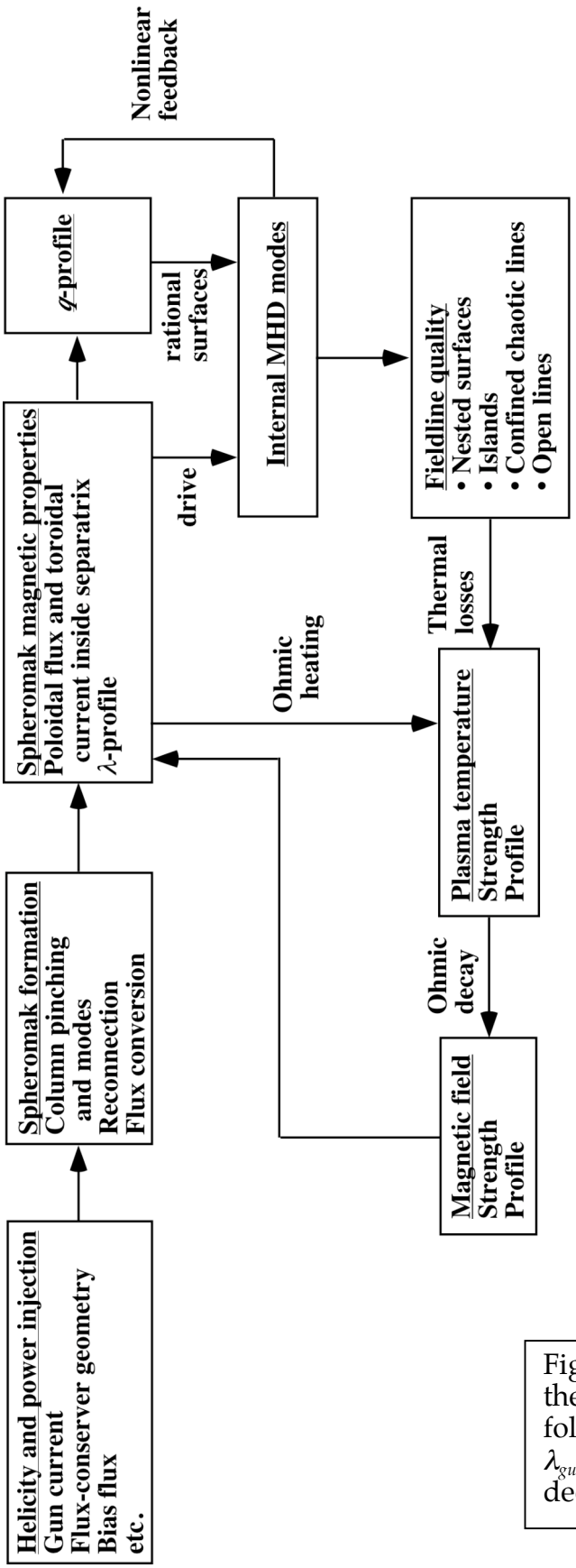

Fig. 7. Interacting processes during the evolution of the spheromak following formation. For the values of λ_{gun} considered here, the spheromak decays following formation.

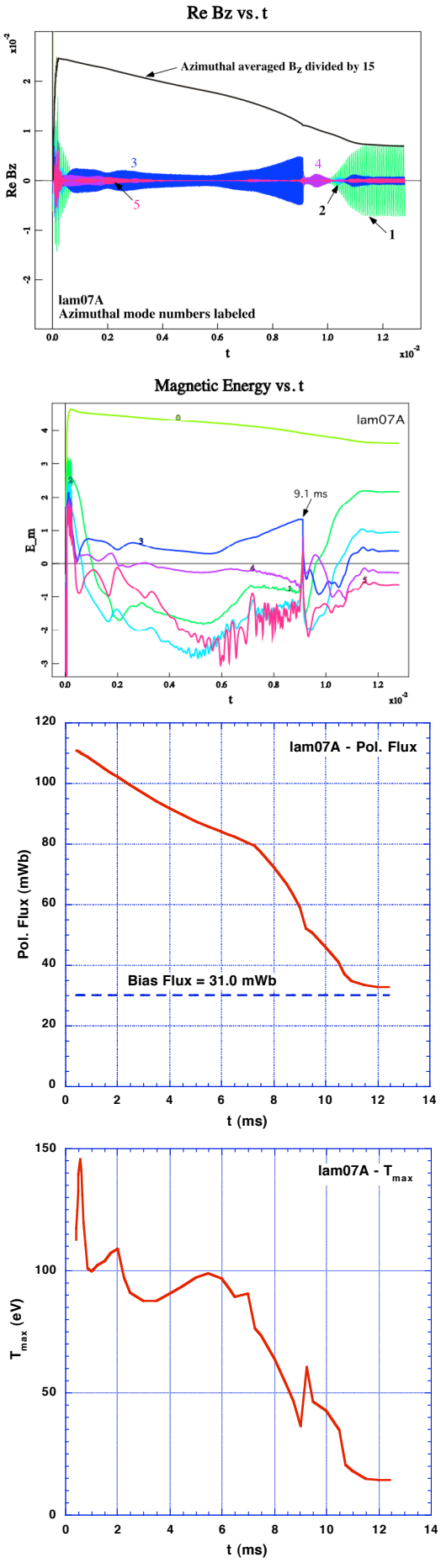

Fig. 8. Evolution of *lam07A*. (a) Magnetic mode activity – poloidal field at the midplane of the flux conserver, labeled by mode-number, n. (Amplitude = $\sqrt{2}$ times ReB_z except for azimuthally-averaged field.) (b) Volume-integrated mode energy, including azimuthally averaged value ($n = 0$). The $n = 3$ mode is the largest non-symmetric magnetic oscillation during most of the discharge. (c) Azimuthally-averaged poloidal flux, asymptoting to the applied bias flux; note the spheromak collapse late in time, followed by the rise of an unstable, n=1 column mode. (d) Peak (azimuthally-averaged) temperature ($T = T_e = T_i$).

At the start of the simulation (0.426 ms) a fairly large volume of good magnetic surfaces has formed and the temperature contours reflect this. The plasma is heated strongly ($T_e = T_i$) with a rate due to $\eta j^2/2$ of 400 eV/ms at a density of $5\text{x}10^{20}$ m^{-3}, temperature 100 eV, and a plasma current of 800 kA. However, the mode evolution during the heating causes a deterioration of the quality of flux surfaces, and by the time of the peak temperature (t = 0.560 ms) many of the surfaces have been destroyed and replaced by stochastic fieldlines. The plasma characteristics for these two times are shown in Figs. 9 and 10. Note that at 0.426 ms the lowest rational surface spanned by the safety factor is ¾ but it has dropped to 2/3 by 0.560 ms.

We explore the mode behavior over this time period in Figs. 11 and 12. In Fig. 11 the energy evolution in time is expanded. We see that the n=1 and 2 modes are decreasing in energy, whereas the n = 3 to 5 are increasing. (Up to 22 modes have been included in the simulation, with no significant qualitative changes.) The mode structures are shown in Fig. 12. The n = 1 and n = 2 modes

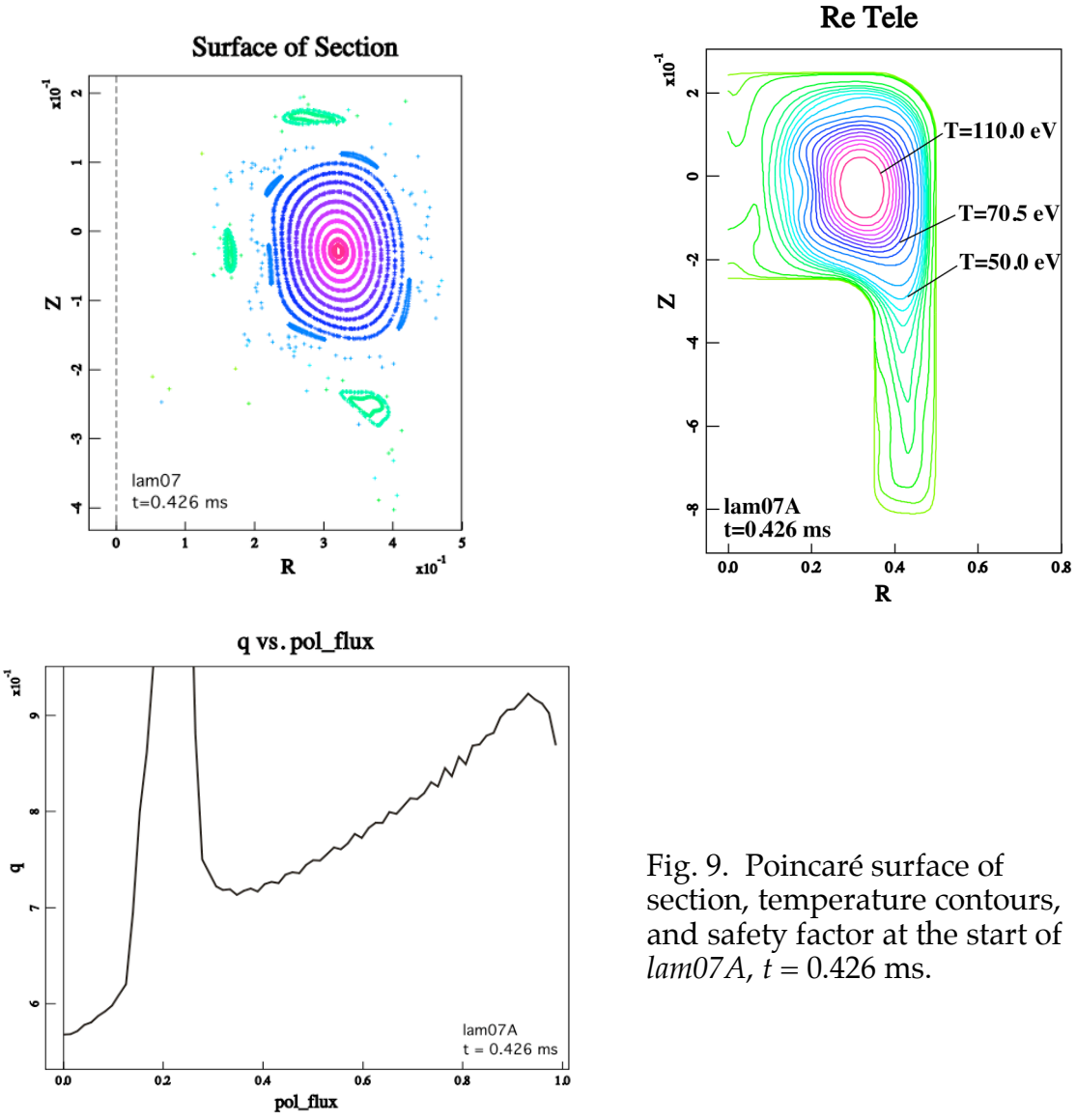

Fig. 9. Poincaré surface of section, temperature contours, and safety factor at the start of *lam07A*, t = 0.426 ms.

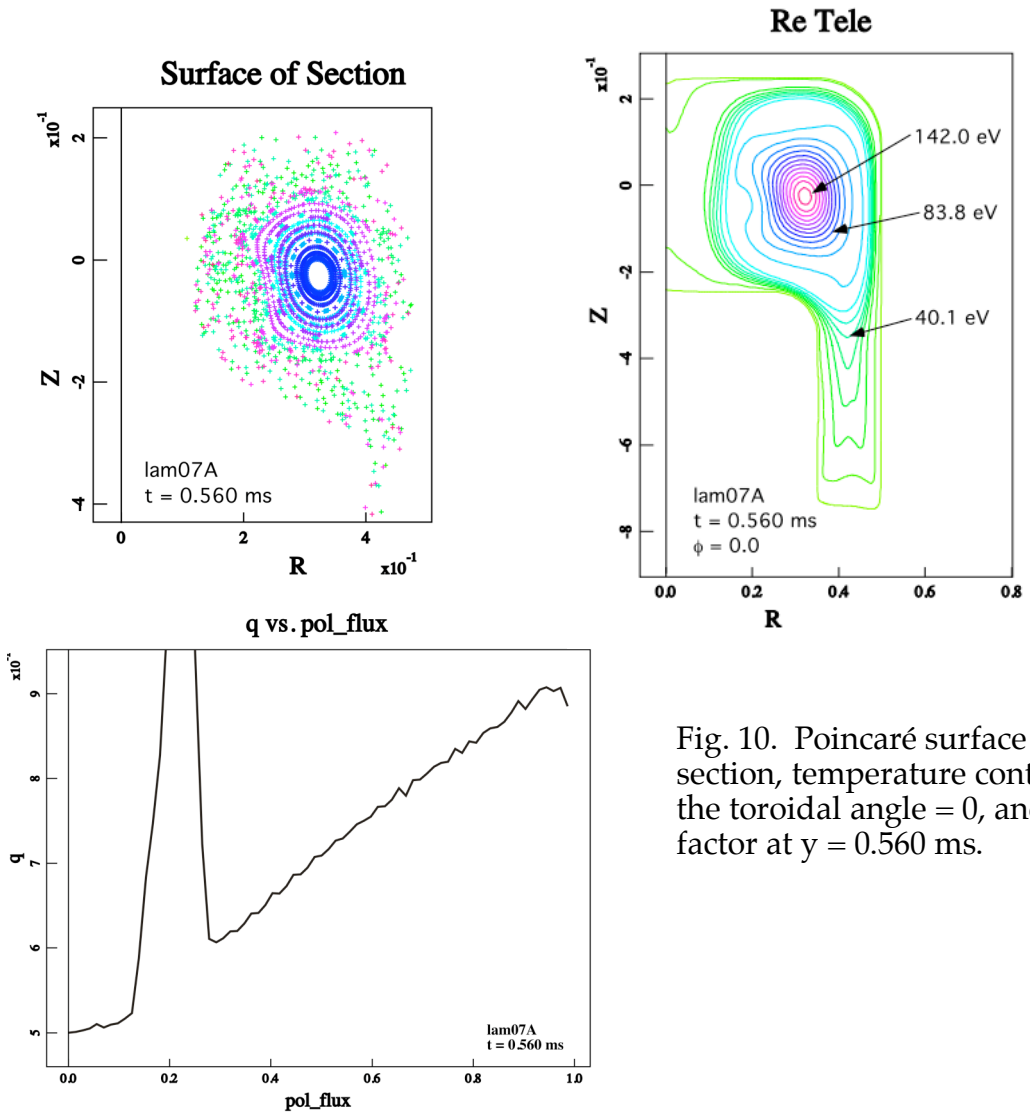

Fig. 10. Poincaré surface of section, temperature contours at the toroidal angle = 0, and safety factor at y = 0.560 ms.

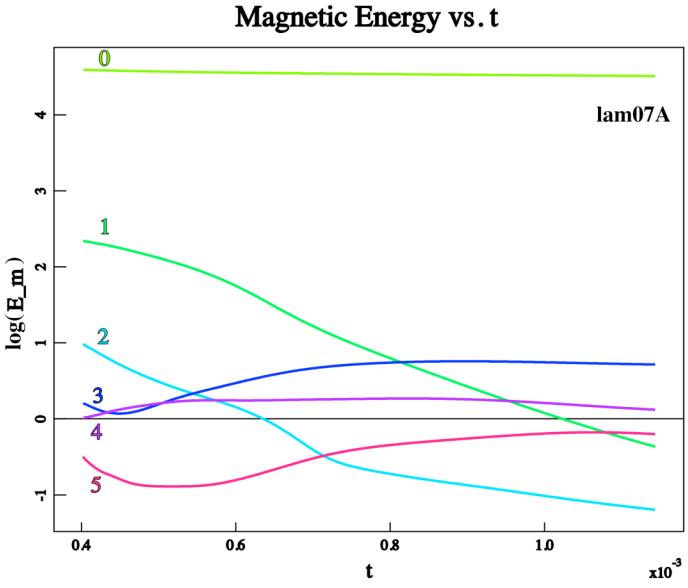

Fig. 11. Expanded time history of the mode energy for *lam07A*. The safety factor, Fig. 10, spans 2/3, 3/4, and 4/5, corresponding to the internal modes at 0.560 ms seen in Fig. 12.

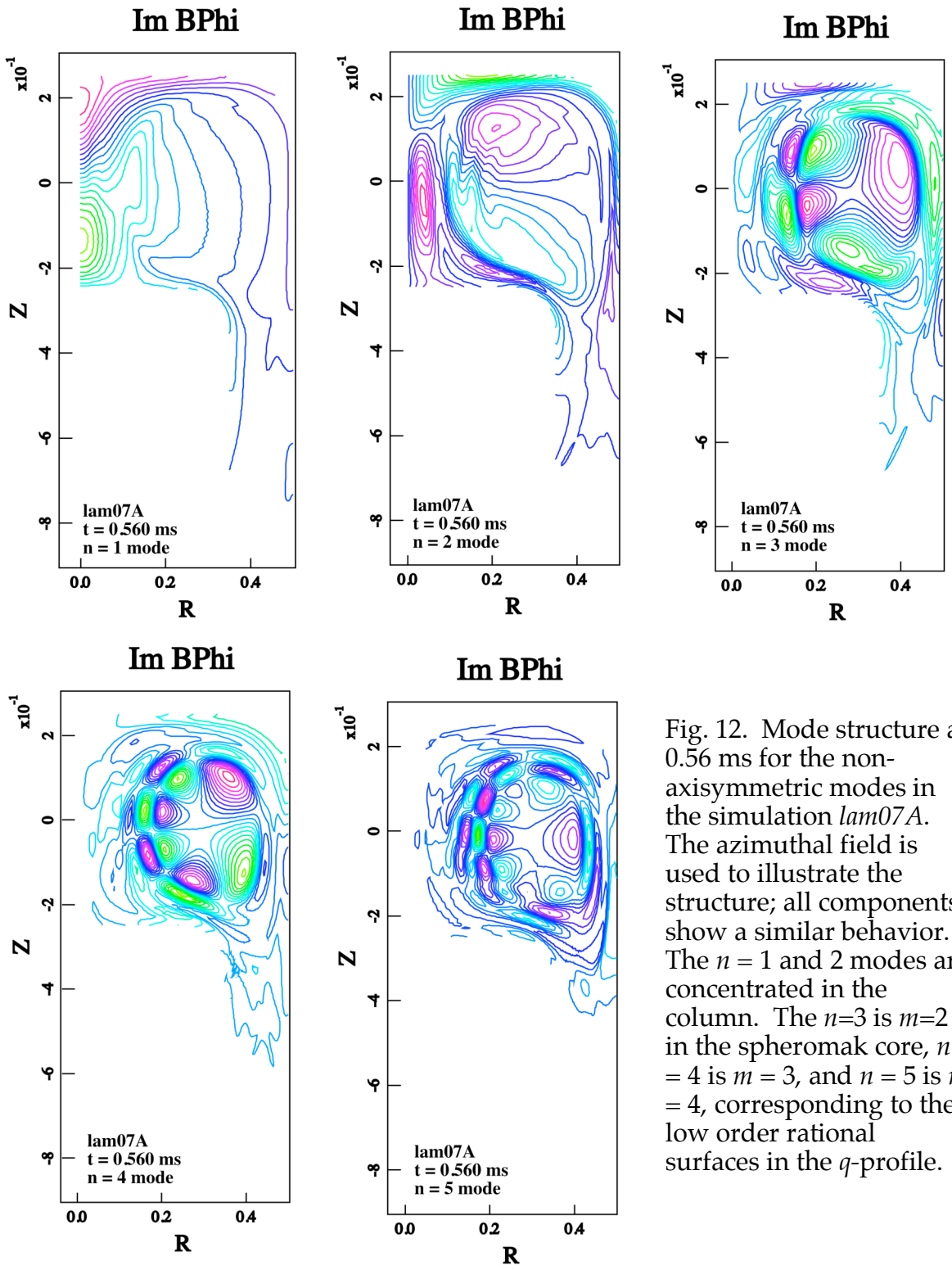

Fig. 12. Mode structure at 0.56 ms for the non-axisymmetric modes in the simulation *lam07A*. The azimuthal field is used to illustrate the structure; all components show a similar behavior. The $n = 1$ and 2 modes are concentrated in the column. The n=3 is m=2 in the spheromak core, $n = 4$ is $m = 3$, and $n = 5$ is $m = 4$, corresponding to the low order rational surfaces in the q-profile.

are large primarily in the flux core region along the geometric axis, consistent with the lack of any q-values (Fig. 10) in the spheromak corresponding to low rational surfaces at $n = 1$ or 2 at 0.560 ms. There are such values for n = 3, 4, and 5, with values 2/3, 3/4, and 4/5, however, and the mode structures reflect this. Note that these modes also vary with minor radius; the peaks at largest minor radius lie on (or just inside) the separatrix.

The magnetic fieldline structure is quite sensitive to these interior modes. In the simplest approximation, the width of an island, Δ, is estimated as

$$\frac{\Delta}{a} \approx \sqrt{\frac{\delta B}{B}\frac{1}{q'a}}$$

with a the minor radius. The width thus scales as the 1/4 power of the mode energy.[a] In our results, $q'a \approx 0.3$ at t = 0.56 ms and $(\delta B/B)^2 \approx 10^{-4}$ (Fig. 8), so $\Delta/a \approx 0.2$. The 2/3 and 3/4 islands have clearly become sufficiently large to overlap and generate the stochastic behavior seen in Fig. 10. It is also noteworthy that the amplitudes of the fields are small near the magnetic axis, as one expects for interior modes, so that there is a core region there which has closed surfaces.

The profile of λ shows considerable structure, looking much like that seen in Fig. 3 for *lam*07. The contour plot seen there shows a region of minimum λ inside the separatrix as well as a minimum on the magnetic axis. It is known that the growth rate for tearing modes is proportional to the gradient in λ,[8] so this may be contributing to the excitation of the modes.

As the plasma current decays, the q-profile evolves as seen in Fig. 13. It typically will "lock" onto a low rational value, 1/2 in the present case. We can also see that as the plasma starts to decay the fraction of poloidal flux inside the separatrix becomes small. This can be compared to the poloidal-flux time-history in Fig. 8; by 12 ms the total poloidal flux has nearly decayed to the applied bias value.

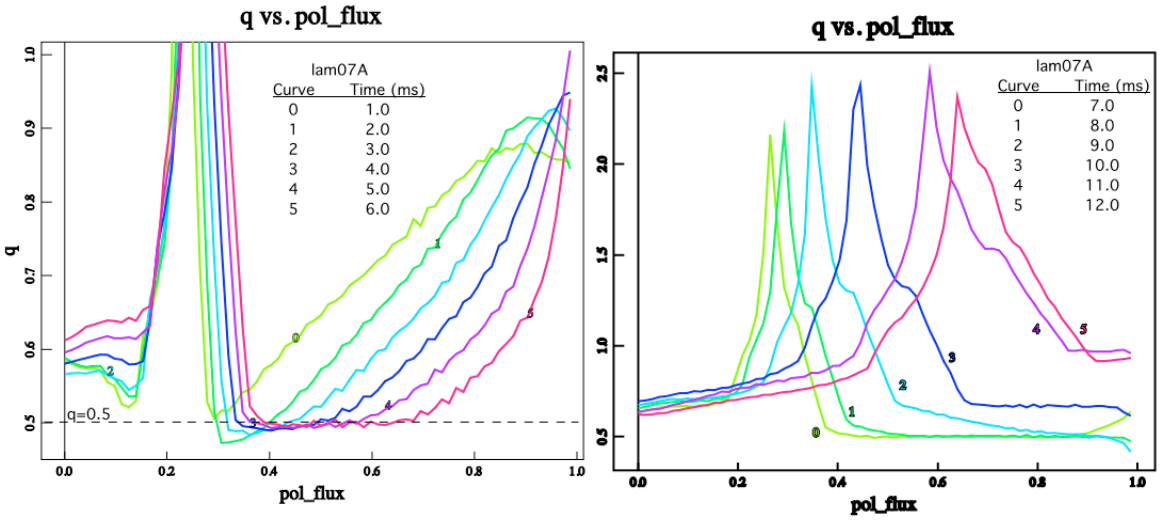

Fig. 13. q-profile evolution from 1.0 to 12.0 ms. The minimum value of q begins to increase at about the time the n = 3 mode amplitude collapses.

At 4.0 ms the interior 2/3 resonance has moved near the magnetic axis. The resulting n=3, m=2 mode structure is shown in Fig. 14. We see evidence for the mode near the core and near the separatrix.

[a]Ken Fowler emphasized the lack of sensitivity of this scaling to me.

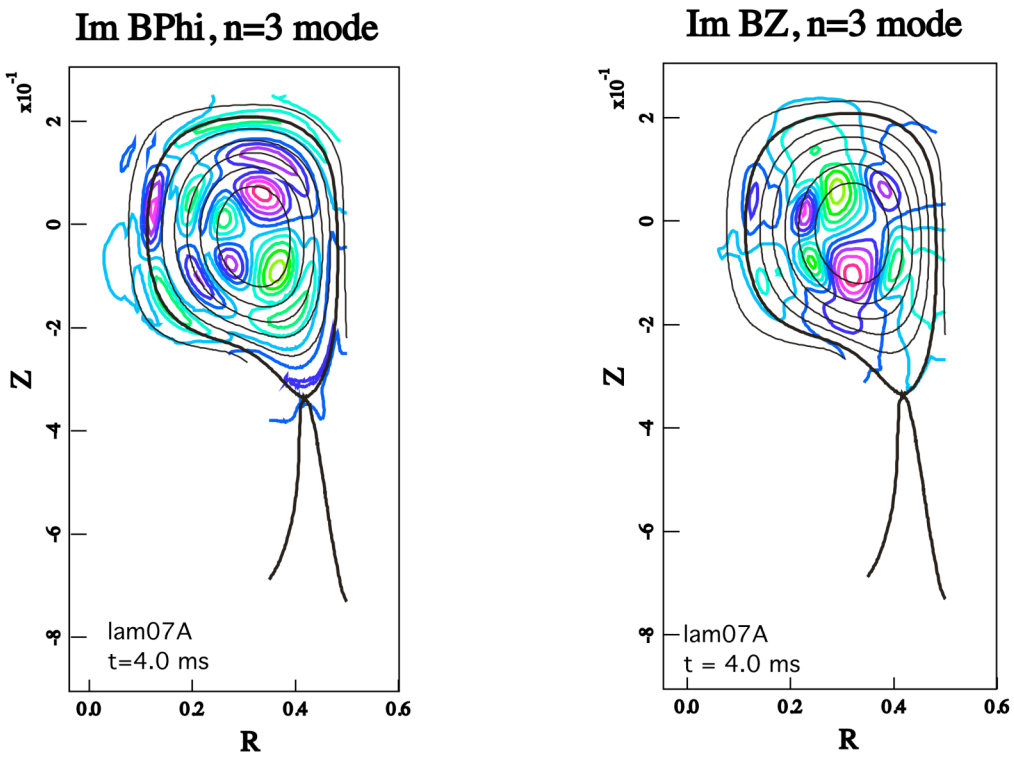

Fig. 14. Mode structure for the n = 3 mode at 4.0 ms and $\lambda_{gun} = 9.0\ m^{-1}$.

The surface of section at 6.0 ms, when the q-profile has a substantial flat section, is quite complex, as shown in Fig. 15, consisting of a central region of closed surfaces, an $m = 2$ island structure, and a considerable volume of stochastic lines which are confined.

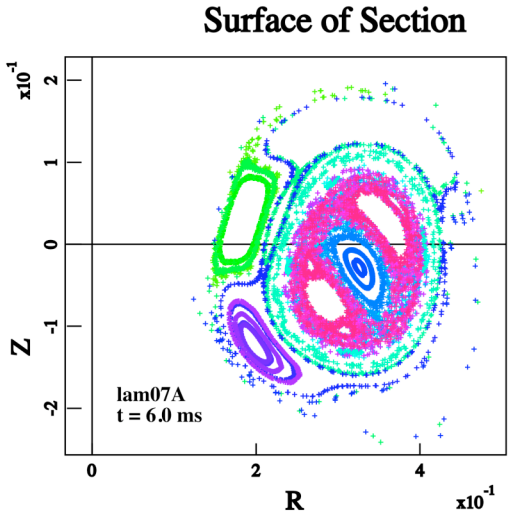

Fig. 15. Surface of section at 6.0 ms. Note that several enclosed areas have not been resolved by the starting points of the fieldline-tracing calculation. The m = 2 structure is apparent in the core.

By 7.0 ms the resonance with the $q = 2/3$ surface has disappeared from the center of the plasma and the only remaining resonances are near the separatrix. The mode structure reflects this, as seen in Fig. 16.

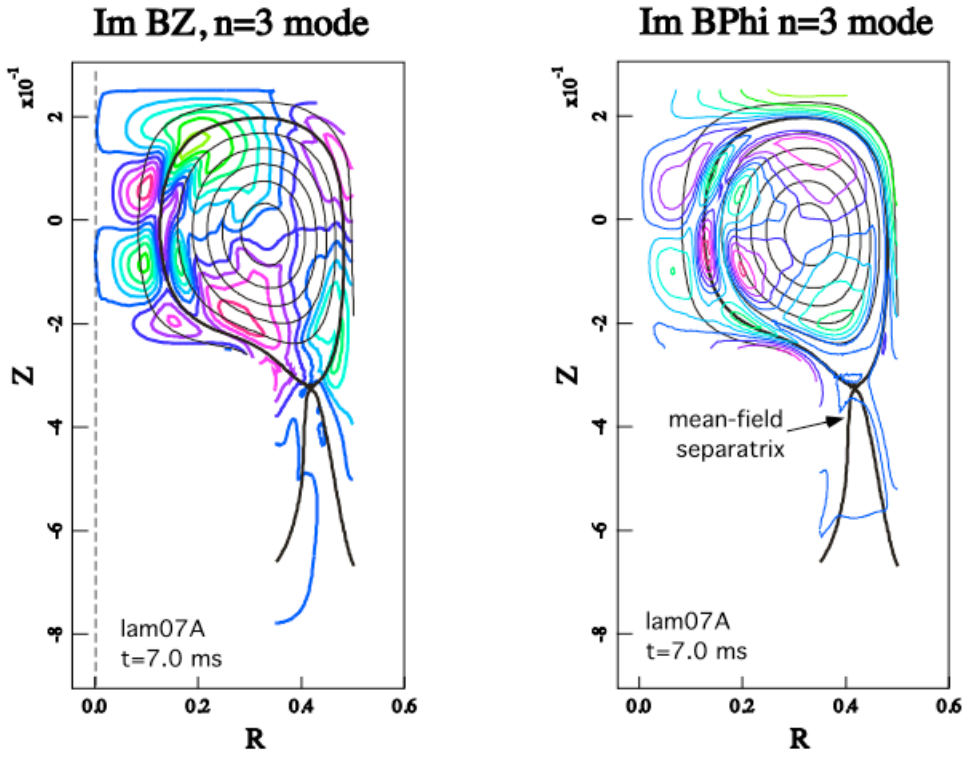

Fig. 16. Structure of the n = 2, m = 3 mode at 7.0 ms for $\lambda_{gun} = 9.0\ m^{-1}$.

Late in time, the poloidal flux has decayed, approaching the bias flux. The observed modes are essentially column modes, as seen from the structure of the $n = 1$ azimuthal magnetic field, Fig. 17.

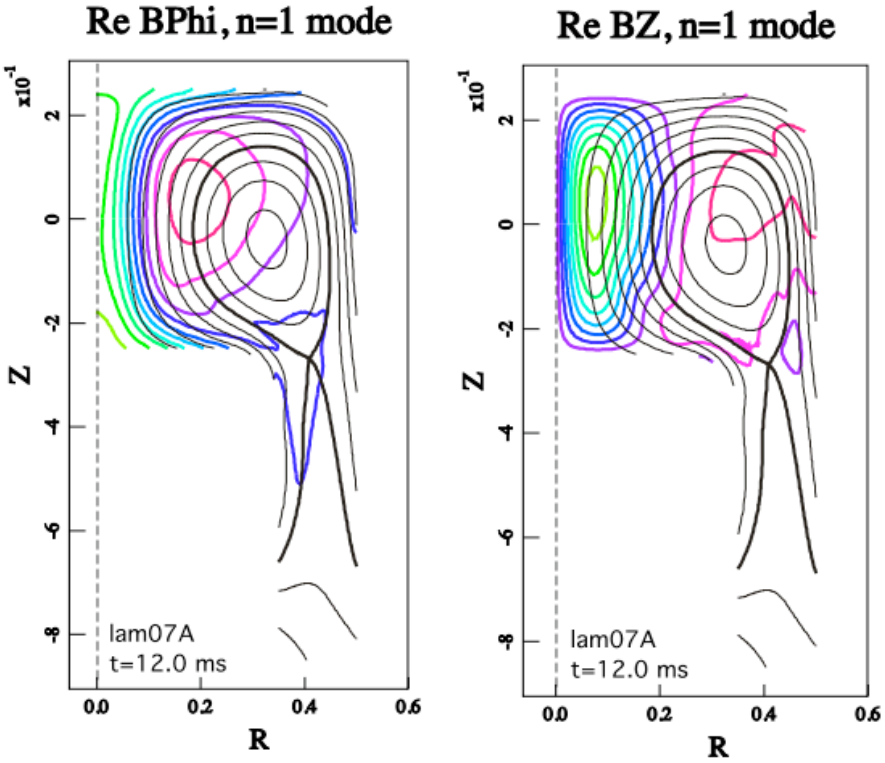

Fig. 17. Magnetic field structure of the $n = 1$ mode late in time when the spheromak poloidal flux has decayed to a low value. The fields are concentrated in the central column. The mean-field separatrix is shown overlaying the mode structure.

Varying λ_{gun}. Given the sensitivity of the internal structure and electron temperature on the detailed q- and λ-profiles, it is perhaps not surprising that there is a corresponding sensitivity to the gun parameters. This can be seen for our simulations in the evolution of the magnetic modes as seen in Fig. 18 and the corresponding peak temperature evolution, Fig. 19. Accompanying all of these are slow decays of the toroidal current and poloidal flux (not shown). As we will see below, this behavior is accompanied by temperature variations, q-profiles, and magnetic field structure, all of which interact in a rather complex manner to generate the differences among these discharges.

Particularly noticeable in the time histories is the relatively slow decay of the spheromak with $\lambda_{gun} = 9.0\ m^{-1}$, close to the experimental value for the peak electron temperature seen in Fig. 1. (After about 9 ms the configuration is essentially a plasma column with little closed mean-flux.) In this case the n = 3 mode is dominant throughout much of the simulation time, whereas it was small at late times for $\lambda_{gun} = 8.6\ m^{-1}$ where the $n = 4$ mode becomes dominant.

The q-profiles at other values of λ_{gun}, Fig. 20, are similar to those in *lam07A.* At lower gun current, *lam07A*, the decay and nonlinear effects have reduced the core value of q much more than seen in Fig. 13, so that the resonance with the 2/3 mode occurs very near the magnetic axis (poloidal flux = 1). (There is also a resonance just inside the separatrix, of course.) At $\lambda_{gun} = 9.9\ m^{-1}$, on the other hand, the amplitude of the n=4 mode is small throughout most of the discharge, and the q-profile has locked onto the 2/3 surface.

There is generally a good correlation between the temperature evolution and the modes. As examples, note the reduced temperature decay rate in *lam07B* between 5 and 9.5 ms when there is only one MHD mode of significant amplitude. Similar effects are seen in *lam07E* and *lam07C*.

V. Discussion

Sensitivity to the q-profile. The sensitivity to the q-profile is seen in other NIMROD simulations, e.g. the simulation of the new capacitor bank being constructed for SSPX.[5,9] When multiple, low-order rational surfaces are found in the profile, corresponding modes are excited and a volume of stochastic magnetic field is generated even though the mode amplitudes are low. The resulting thermal conduction essentially flattens the electron temperature in this volume. The experiment appears to show similar effects, although there is no direct measurement of the fieldline structure. It is clear that the generation of long-term confinement will require a feedback or other mechanism to maintain good surfaces.

Can we use the gun current for feedback control? With SSPX as presently configured, the poloidal flux is frozen into the walls and the only mechanism for feedback is to vary the gun current. Given the sensitivity to the q-profile, it is reasonable to consider the possibility of modifying it to limit the number of modes that are excited, and thus affect the presence or volume of stochastic fieldlines. We consider the possibility of using this for feedback; numerical consideration will be undertaken in a future campaign.

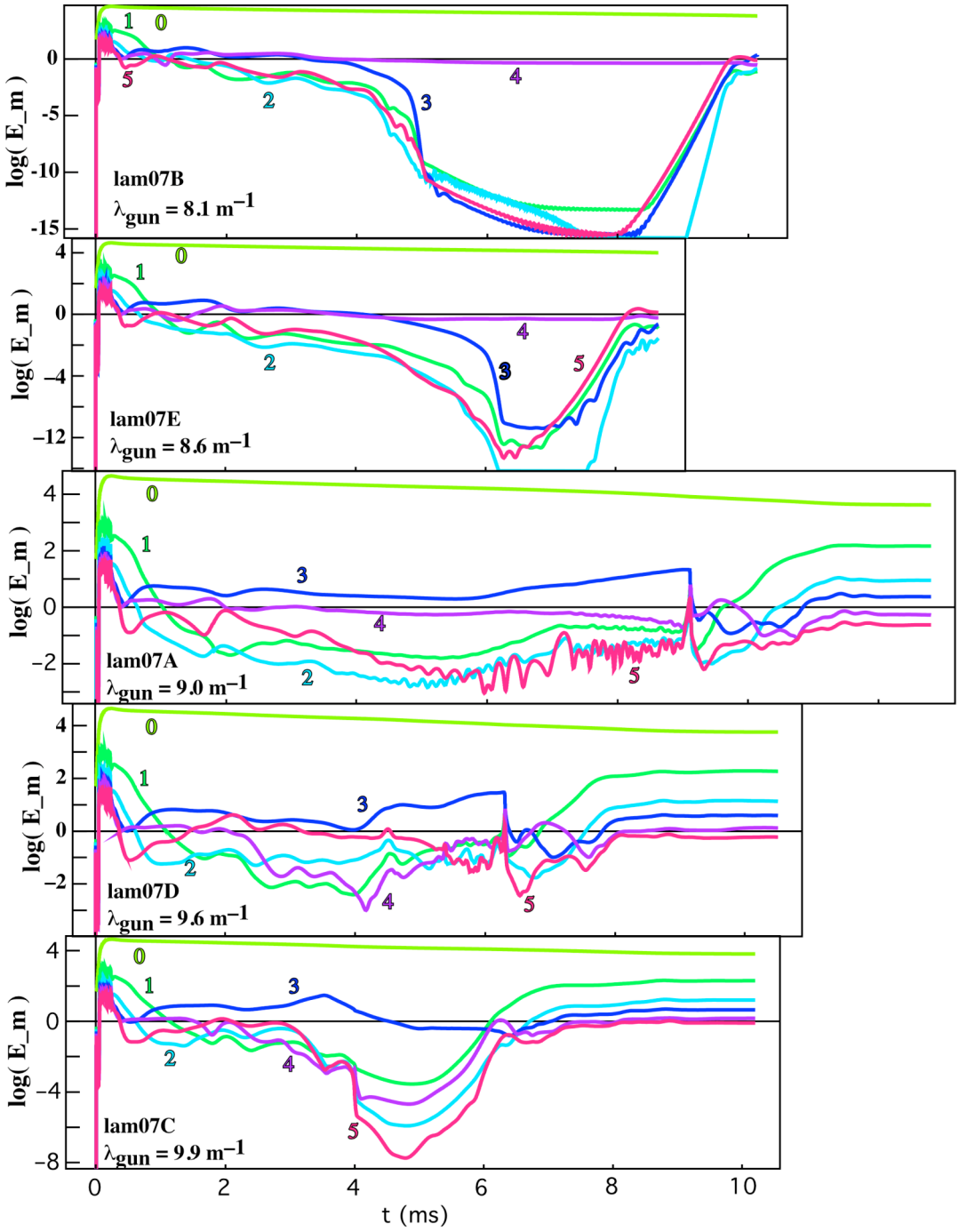

Fig. 17. Variation in the time evolution of the spheromak modes as a function of λ_{gun}. Note the differences in the energy scales. The runs were not all ended at the same time.

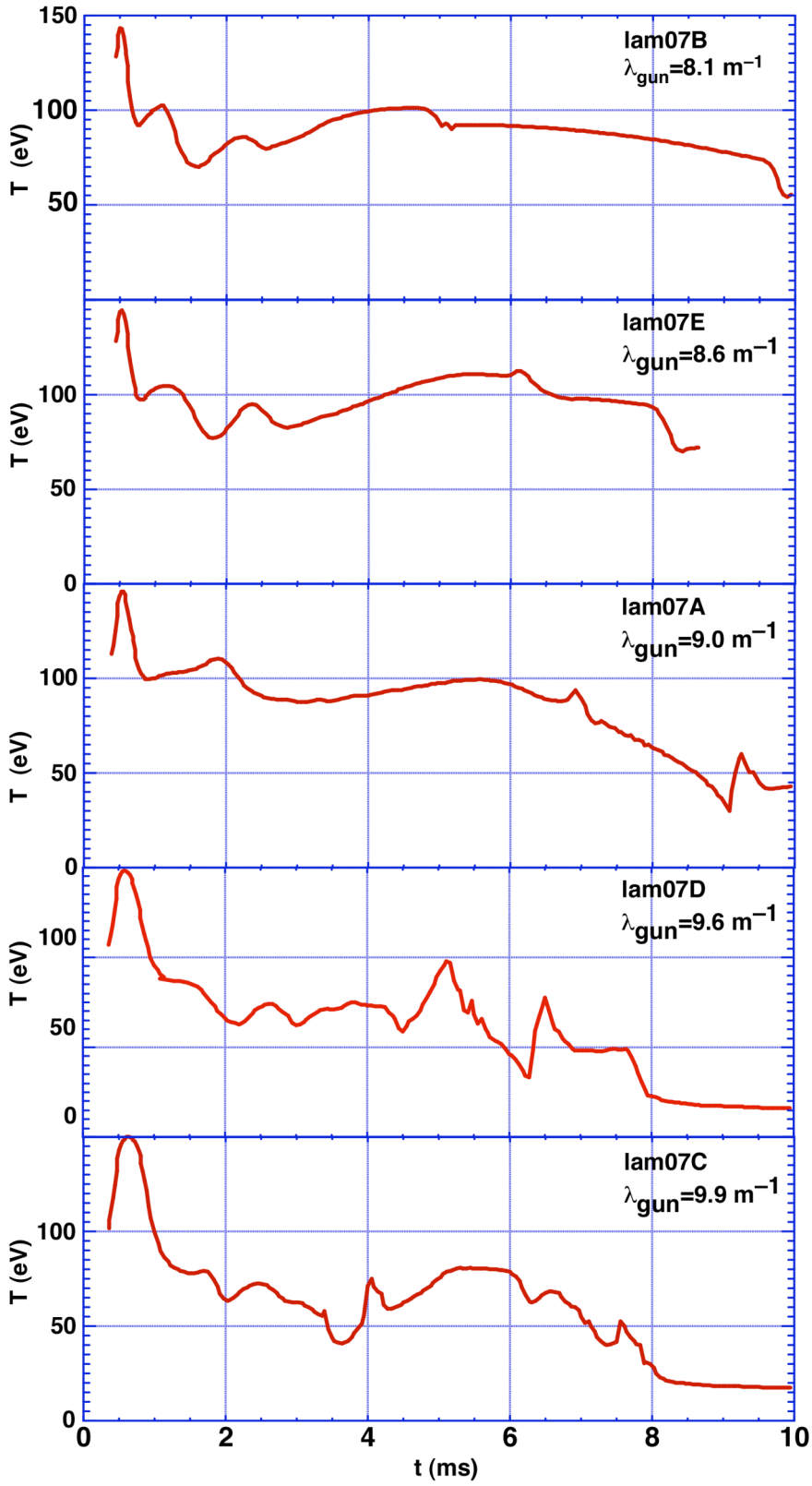

Fig. 18. Peak temperature (n = 0) evolution as a function of λ_{gun}.

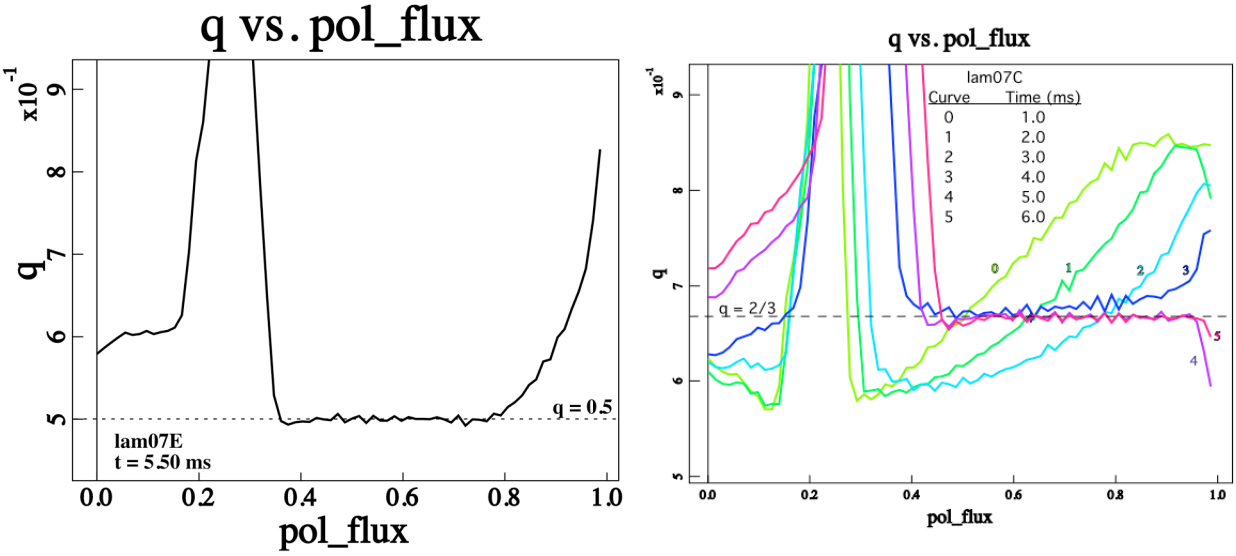

Fig. 19. Safety factor for $\lambda_{gun} = 8.6$ m^{-1} at 5.5 ms (left) and for $\lambda_{gun} = 9.9$ m^{-1} at several times (right).

Consider the "cylindrical" safety factor as an approximation to q:

$$q_c = rB_\varphi / RB_p$$

with r and R the minor and major radii. In the same approximation the toroidal field on the horizontal axis is

$$B_\varphi = \frac{\mu_0 I_p}{2\pi R} = \frac{\mu_0}{2\pi R}\left[I_{gun} + 2\pi \int_{R_s}^{R} j_z(r, z=0) R dR\right]$$

and

$$B_p = \frac{\mu_0}{r}\int_0^r j_\varphi(r, z=0) r dr$$

so

$$q_c = \frac{r^2}{2\pi R^2}\frac{\left[I_{gun} + 2\pi \int_{R_s}^{R} j_z(r, z=0) R dR\right]}{\int_0^r j_\varphi(r, z=0) r dr}$$

To the extent that the currents inside the separatrix are not affected by a change in the gun current, δI_{gun}, it causes a change in the q-profile

$$\delta q_c = \frac{r^2}{2\pi R^2}\frac{\delta I_{gun}}{\int_0^r j_\varphi(r, z=0) r dr}$$

The actual change in profile depends on the distribution of toroidal current. If j_φ is constant the profile is raised or lowered by

$$\delta q_c = \frac{1}{2\pi R^2}\frac{\delta I_{gun}}{j_\varphi}$$

In the long-thin approximation, this is only weakly dependent on the minor radius. In the actual spheromak, however, the aspect ratio is close to unity, so the dependence will still be moderately large. In general, the net effect will also depend on the details of the current distribution, on toroidal effects and on inductive or transport changes in the currents inside the separatrix. Separating all these effects will require considerable computational effort.

Acknowledgements

Bruce Cohen and Carl Sovinec have made significant contributions to this work, both in helping me to carry it out and in discussions about the physics of the results.

References

1. R. D. Wood, B. I. Cohen, D. N. Hill, E. B. Hooper, R. H. Cohen, S. Woodruff, H. S. McLean, L. L. LoDestro, L. D. Pearlstein, D. D. Ryutov, B. W. Stallard, and M. V. Umansky, "Improved Operation and Modeling of the SSPX Spheromak," submitted to Nucl. Fusion (2005).
2. C. R. Sovinec, B. I. Cohen, G. A. Cone, E. B. Hooper, and H. S. McLean, "Numerical Investigation of Transients in the SSPX Spheromak," Phys. Rev. Letters **94**, 035003 (2005).
3. B. I. Cohen, E. B. Hooper, R. H. Cohen, D. N. Hill, H. S. McLean, R. D. Wood, S. Woodruff, C. R. Sovinec and G. A. Cone, "Simulation of spheromak evolution and energy confinement," Phys. Plasmas **12**, 056106 (2005).
4. E. B. Hooper, T. A. Kopriva, B. I. Cohen, D. N. Hill, H. S. McLean, R. D. Wood, S. Woodruff, "A magnetic reconnection event in a driven spheromak," Phys. Plasmas, to be published.
5. Bick Hooper and Bruce Cohen, "Magnetic topology: Its evolution and consequences in SSPX," NIMROD Team Meeting, August 9-10, 2005, Madison, WI. (UCRL-PRES-214111).
6. H. S. McLean, et al., to be published.
7. D. A. Kitson and P. K. Browning, "Partially Relaxed Magnetic Field Equilibria in a Gun-Injected Spheromak," Plasma Phys. Controlled Fusion **32**, 1265 (1990).
8. Allen H. Boozer, "Plasma Confinement," *Encyclopedia of Physical Science and Technology* (Academic Press, Inc., 1992), Vol. 13.
9. B. I. Cohen, E. B. Hooper, and C. R. Sovinec, "NIMROD Simulation of SSPX Spheromak Physics," presented at the 2005 International Sherwood Theory conf., Stateline, NV, April 11-13, 2005 (UCRL-PRES-211322).